

## Low-frequency strain sensor using a fiber Bragg laser

E. MACCIONI<sup>(1)(2)(3)</sup>, N. BEVERINI<sup>(1)(2)(3)</sup>, M. MORGANTI<sup>(1)(2)</sup>, F. STEFANI<sup>(2)</sup>,  
R. FALCIAI<sup>(4)</sup> and C. TRONO<sup>(4)</sup>

<sup>(1)</sup> *Dipartimento di Fisica "E. Fermi", Università di Pisa - Largo B. Pontecorvo 2  
56127 Pisa, Italy*

<sup>(2)</sup> *INFN, Sezione di Pisa - Largo B. Pontecorvo 2, 56127 Pisa, Italy*

<sup>(3)</sup> *Consorzio Nazionale Interuniversitario per le Scienze fisiche e della Materia (CNISM)  
Sezione di Pisa - Largo B. Pontecorvo 2, 56127 Pisa, Italy*

<sup>(4)</sup> *Istituto di Fisica Applicata "N. Carrara", IFAC-CNR - Via Madonna del Piano 2  
50019 Sesto Fiorentino, Firenze, Italy*

(ricevuto il 27 Dicembre 2007; approvato il 9 Gennaio 2008; pubblicato online l'8 Aprile 2008)

**Summary.** — We have developed a Fiber Laser Strain Sensor (FLSS) which shows noise-equivalent sensitivity equal to or better than  $150 \text{ p}\epsilon_{\text{r.m.s.}}/(\text{Hz})^{1/2}$  at very low frequencies, from 50 mHz to several tens of Hz. The strain acts on the fiber laser emission wavelength, and an imbalanced Mach-Zender Interferometer (MZI) converts wavelength variations into phase-amplitude variations. In the time domain the device shows a good signal-to-noise ratio also at the lowest tested frequency of 50 mHz, with a resolution better than  $1 \text{ n}\epsilon_{\text{r.m.s.}}$ . The device can find application in many fields, primarily in geological prospecting and in monitoring of civil structures.

PACS 07.10.Pz – Instruments for strain, force, and torque.

PACS 07.60.Vg – Fiber-optic instruments.

PACS 42.55.Wd – Fiber lasers.

### 1. – Introduction

Devices based on Fiber Bragg Lasers (FBLs) have demonstrated sensitivity at the level of few tens of femto-strain for signals in the kHz bandwidth [1], and their potentiality as acoustic sensors in water has already been exploited up to 100 kHz [2-4]. For a lot of applications (monitoring of civil structures, rock deformation probing, seismic and geodynamical monitoring) there is a growing interest in strain sensors in "quasi-static" regime (0.001–100 Hz). In this frequency region, acoustic noise, local temperature fluctuations and air movements are the limiting factors to the attainable sensitivity. In geological prospecting, very long period strain measurements are accomplished essentially by means of borehole strain-meters. The physical principle of these instruments rests on the capacitive transduction of the strain acting on the walls of the well. The device can provide three-axial reconstruction of the strain wave with a long-term (months)

sensitivity better than  $1 \text{ n}\epsilon$ . The deployment of the system is however cumbersome and expensive, requiring the excavation of a deep well (several hundred meters); also the sensor itself has a quite high cost, and it cannot be any more recovered, when cemented in the well. Moreover the detection is limited to a small region around the bottom of the well and needs electrical cabling of the hole. If we pay our attention to more superficial phenomena and to events of shorter characteristic period, as strain in rock layers or during micro-seismic activity, alternative low-cost sensors are needed. In this field, next-generation devices are fiber optic strain-meters, as those based on Fiber Bragg Gratings (FBG) [5], in-Fiber Fabry-Perot resonators (FFP), and, above all, Fiber Bragg Lasers (FBL). A sensitivity of  $1.2 \text{ n}\epsilon/(\text{Hz})^{1/2}$  was reached at 1.5 Hz by remote interrogation of a FBG through an external-cavity diode laser [6]. In another work [7,8], a highly sophisticated stabilized laser system, using a Pound-Drever-Hall frequency locking scheme, was employed in remote interrogation of a FFP, formed by a pair of separated FBG. With this technique sensitivity better than  $1 \text{ p}\epsilon/(\text{Hz})^{1/2}$  beyond 100 Hz, and of  $6 \text{ p}\epsilon/(\text{Hz})^{1/2}$  around 100 Hz was attained.

In this paper we present a Fiber Laser Strain Sensor (FLSS) devoted to very low frequency measurements, with a noise-equivalent sensitivity better than  $150 \text{ p}\epsilon_{\text{r.m.s.}}/(\text{Hz})^{1/2}$  from about 50 mHz to 7 Hz. A resolution better than  $1 \text{ n}\epsilon_{\text{r.m.s.}}$  is achieved for wide-band time-domain acquisitions of sinusoidal strain signals for a frequency down to 50 mHz.

## 2. – Experimental set-up

The use of distributed Bragg reflector fiber lasers as very sensitive sensors has been already described elsewhere [2,9]. Our lasers work with about 200 mW of 980 nm pumping power, generating about 0.5 mW of single-frequency radiation around 1533 nm [3,4]. The laser cavity output coupler FBG (reflectivity about 90%) is oriented towards the pump beam direction, so that the larger part of the FBL power is emitted backwards. In this way, a single optical fiber can connect the sensor with the remote position where the pump laser and the FBL radiation detection system are positioned. The other FBG is almost totally reflecting and is photo-imprinted about 2 cm apart, so that the two Bragg gratings form a Fabry-Perot cavity. The exact FBL wavelength is determined by the optical length of this cavity, which is sensitive to external perturbation due to strain, pressure or temperature variations through its elastic constants, thermal coefficient and stress-optic tensor [10-12]. A high-sensitive detection of these wavelengths variations is obtained by an interferometric method, using an imbalanced in-fiber Mach-Zender Interferometer (MZI) that converts wavelengths variations into intensity variations [13]. Calibrated strains can be applied to the FLSS by a piezo-electric stretcher fixed to a fiber end. The transduction factor of the piezoelectric stretcher was measured experimentally as

$$(1) \quad \frac{\delta\epsilon}{\delta V} = 19 \pm 2 \text{ n}\epsilon/\text{V}.$$

At very low frequency, a particular care must be devoted to distinguish between strain response and thermal effect: note that a temperature variation of the order of  $0.1^\circ\text{C}$  has the same effect of one micro-strain lengthening. A passive insulation of the FLSS makes thermal perturbations negligible down to some tens of mHz. In order to operate with the MZI output signal always in the linear region, and close to its maximum responsivity, we have locked its imbalance length to the FBL emission wavelength: a servo control with a

Fig.  
enck  
phot  
the 1

time  
MZI  
low  
data  
1  
large  
satu  
air t  
fiber  
with  
insu

3. –

T

(2)

when  
fract  
A is  
visib  
ment

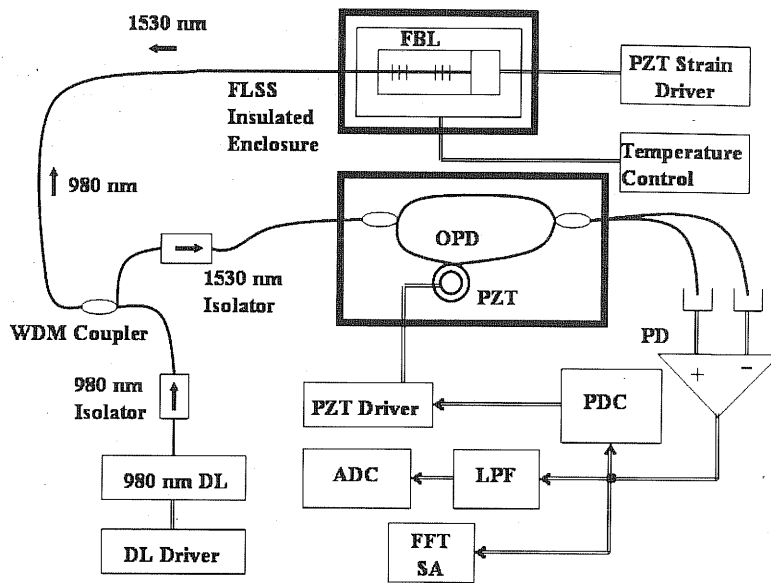


Fig. 1. – The experimental set-up with the FLSS device and the MZI inside their insulated enclosures. FBL is the fiber Bragg laser; OPD is the optical path difference; PDs are the photodiodes; PDC is the phase drift control; LPF is the low-pass frequency filter; FFT-SA is the Fast Fourier Transform spectrum analyzer.

time constant of the order of 30 s drives a fiber piezo actuator stretching one arm of the MZI [3, 4]. By way of this solution, we have been able to observe strain response to very low frequency (50 mHz) without any external adjustment of the stab-lock circuit during data collection. Figure 1 shows the experimental apparatus.

The FBL is positioned in a thermal controlled aluminum housing in order to prevent large laser wavelength drifts, due to long-period temperature variations; in this way saturation of the MZI actuator dynamic range is avoided. A double wooden box shields air turbulences and insulates the device from environmental acoustic noise. The total fiber length on which the strain is applied is 13 cm. A pre-strain is applied to the fiber with a micro-metric screw. The optical signal is sent to the MZI, carefully thermally insulated, and then detected by a couple of photodiodes in balanced configuration.

### 3. – Working principle

The MZI output intensity can be expressed as [14]

$$(2) \quad I(\lambda) = A \{1 + k \cos[\psi(\lambda) + \phi]\},$$

where  $\psi(\lambda) = 2\pi \frac{\text{OPD}}{\lambda}$  (OPD =  $nL$  is the Optical Path Difference,  $n$  is the fiber core refractive index and  $L$  is the length difference between the two arms of the interferometer).  $A$  is proportional to the MZI input intensity and system losses,  $k$  is the interferometric visibility, and  $\phi$  is the MZI bias phase offset, varying slowly and randomly with environmental conditions. When a strain at frequency  $f$  of the kind  $\varepsilon \sin(2\pi ft)$  modulates the

emission wavelength, we have for the phase variation [15]:

$$(3) \quad \Delta\psi(t) = 2\pi \frac{OPD}{\lambda} (1 - P_e) \varepsilon \sin(2\pi ft),$$

where  $P_e$  is the effective photo-elastic constant for fused silica ( $P_e \approx 0.22$ ).

Note that the phase responsivity is directly proportional to the MZI OPD. For an OPD = 1 m, a numeric evaluation of (3) gives a phase to strain responsivity of

$$(4) \quad \frac{\delta\psi}{\delta\varepsilon} = 2 \mu\text{rad}/\text{p}\varepsilon \quad (\text{OPD} = 1 \text{ m}).$$

The spectral quality of the fiber laser and its intensity noise do not set a limit in allowing micro-radians resolution [16], so that from (4) sub-pico-strain sensitivity would seem obtainable with an OPD of few meters. Effectively, we measured an emission line-width below 5 kHz with an intensity noise lower than 1%. The Relative Intensity Noise (RIN) is further rejected as common-mode noise by balanced photo-detection technique. A noise contribution should come from the thermal phase fluctuations of the in-fiber MZI [17], even if we have tried to insulate it at best from the environment.

However in the frequency range 0–3 kHz and for an OPD of 15 m, this phase noise is only a fraction of  $\mu\text{rad}/(\text{Hz})^{1/2}$  [17] and it does not limit our present sensitivity. The Rayleigh-scattering-induced back-reflection on the fiber laser is a more important phase noise source and it can limit the possibility of placing the sensor far from the detecting interferometer for remote detection. A noise analysis about interferometric detection in fiber optic devices can be found in [16]. At very low frequencies ( $f \leq 1 \text{ Hz}$ ) the  $1/f$  noise becomes the principal limit for the performances. In our set-up we have chosen OPD = 15 m as a compromise between the needs of high sensitivity and good signal stability. In our apparatus the low-frequency limit was fixed at about 30 mHz by the time constant of the opto-electronic servo loop acting on the MZI. The spectral response at various frequencies was tested, by applying a sinusoidal voltage waveform to the FLSS piezo-stretcher and detecting the signal on a FFT spectrum analyzer. Alternatively, the signal is sent to a digital oscilloscope through a low-pass filter for acquisitions in time domain. No significant output voltage drift was observed during a continuous operation of some hours.

#### 4. – Results

Figure 2 yields the power spectral density signal for a  $3 \text{ n}\varepsilon_{\text{r.m.s.}}$  calibration strain at 50 mHz. The feedback loop frequency cut-off at about 30 mHz is clearly visible. Note that the attack point of the feedback loop is not sharp and so the background roll-off is evident in all the frequency range up to 0.5–0.7 Hz. Figure 3 shows the spectrum of a  $0.3 \text{ n}\varepsilon_{\text{r.m.s.}}$  calibration strain at 7 Hz. From the Signal-to-Noise-Ratio (SNR) we can deduce a strain sensitivity of about  $150 \text{ p}\varepsilon/(\text{Hz})^{1/2}$  at 50 mHz and of  $3 \text{ p}\varepsilon/(\text{Hz})^{1/2}$  at 7 Hz.

The FLSS response in the time domain is shown in fig. 4, when a  $3 \text{ n}\varepsilon_{\text{r.m.s.}}$  amplitude sinusoidal excitation is applied at 50 mHz (20 s period). A low-pass frequency filter is provided, with 0.3 Hz band. The sensitivity estimated from fig. 4 is apparently worse than the expected one, on the base of the PSD acquisition of fig. 2. From this PSD measurement it is however evident that the system responsivity is rapidly decreasing from 500 mHz to 50 mHz, due to the feedback loop roll-off and to the elastic and mechanical

Fig.  
sinus

char.  
the c  
RC l  
stati  
that  
unch  
 $10^{-5}$

Fig. 1  
applic

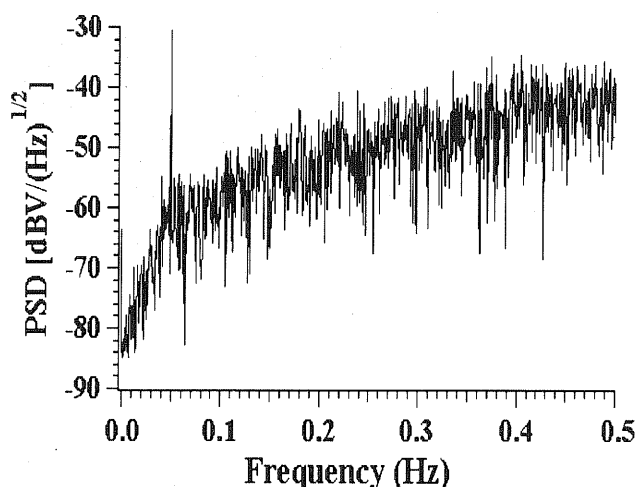


Fig. 2. - Strain spectrum (Power Spectral Density) of the MZI output signal when a  $3\text{ n}\epsilon$  sinusoidal strain at  $50\text{ mHz}$  is applied to the fiber laser.

characteristics of the present device. As a consequence, the noise level is dominated by the contribution of the highest frequencies that are not efficiently filtered by our simple RC low-pass filter. In any case, fig. 4 shows the capability of the system to detect quasi-static sub-nano-strain signals in the time domain. The feature of fig. 4 demonstrates also that, during the total acquisition time of  $100\text{ s}$ , the signal amplitude remains substantially unchanged, and this is both a piece of evidence of temperature stability at the level of  $10^{-5}\text{ }^{\circ}\text{C}$  and that the system is free from laser intensity instabilities in this time period.

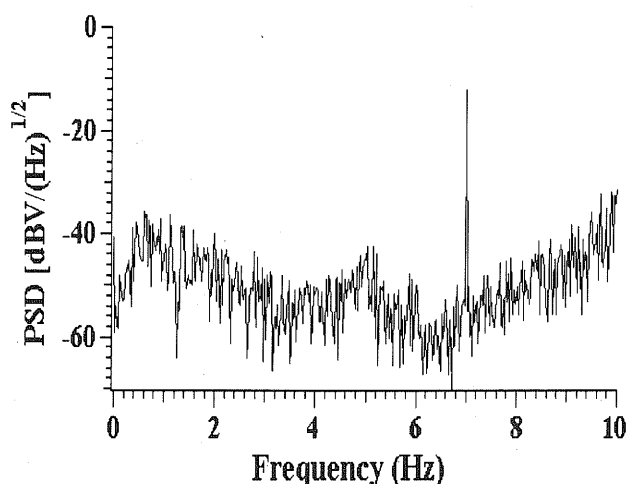


Fig. 3. - Strain spectrum of the MZI output signal when a  $0.3\text{ n}\epsilon$  sinusoidal strain at  $7\text{ Hz}$  is applied to the fiber laser.

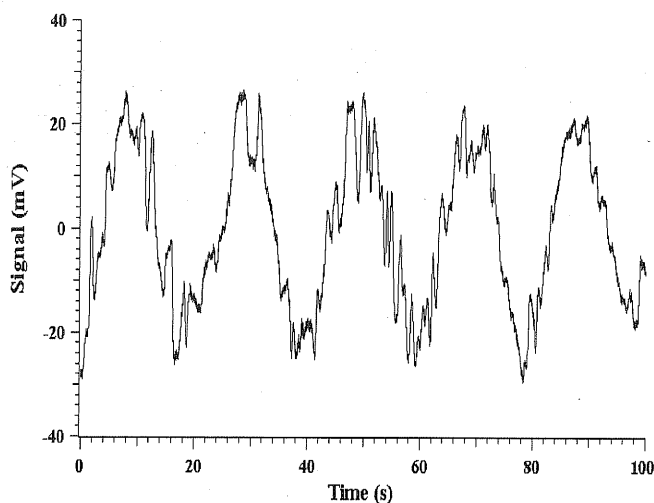


Fig. 4. – The device output signal as a function of the time in the case of a sinusoidal strain wave excitation. Wave frequency of 50 mHz and 3 nε amplitude, observed through a 0.3 Hz low-pass filter.

## 5. – Geophysical applications

Geodesy and seismology ask for precise measurements of the horizontal and vertical movements of a surface reference point with respect to an underground position, during crustal deformations. Fiber optic strain-meters have been developed in the last twenty years and the most precise devices rest upon interferometric detection techniques [18]. Long-term surface displacements (seasonal periods) can exceed some hundreds of micrometers, while vertical movements up to few tens of nanometers are more typical of the natural background noise of the crustal plate, on a frequency scale ranging from tens of mHz to some Hz. In local areas, horizontal and vertical displacements can be simultaneously recorded, to give a full map of the crustal deformation in the event, for example, of micro-seismic activity. Our strain sensor could be implemented to fit well this last need, having showed the appropriate resolution on the required frequency scale (time periods up to some tens of seconds). Different kinds of strain measurements, based on the fiber laser strain sensor, could be undertaken, referencing surface benchmarks to depth through borehole technique or considering superficial rocks displacement by means of less cumbersome versions of the strain gauge itself. The capability of fiber lasers to be photo-imprinted on an optical fiber to form an array of sensors (which can be interrogated from a single remote station) constitutes a strong point, making them good candidates in meeting geophysics requirements.

## 6. – Conclusions

We have shown as an Erbium-doped fiber laser can be the core element of a quasi-static strain sensor. Such a device presents some of the typical advantages of fiber sensors, first of all the possibility to be multiplexed and we are just working to build an array of four FLSS on the same optical fiber, pumped by a single diode laser. Moreover the imbalance of the MZI can be adapted to fit specific needs of sensitivity and measurement

dynamic range. Even two or more interferometers with different OPDs can be used in parallel to cover large strain spans, so that whichever strain amplitude could fall in the operative range of one MZI. We have proven sub-Hz noise-equivalent sensitivity at the level of tens of  $\text{p}\epsilon/(\text{Hz})^{1/2}$  and we have shown sub-nano-strain quasi-static responsivity in the time domain. These performances can be improved with a better acoustic shielding of the receiving MZI, together with a more evolved opto-electronic control of the fringe stabilization system. The demonstration of the FLSS operative principle and the results we have obtained can be the basis to develop sensors suitable to all the situations where slowly varying strain measurement is required.

## REFERENCES

- [1] KOO K. P. and KERSEY A. D., *J. Lightwave Technol.*, **13** (1995) 1243.
- [2] HILL D. J., NASH P. J., JACKSON D. A., WEBB D. J., O'NEIL S. F., BENNION I. and ZHANG L., *Proc. SPIE*, **3860** (1999) 55.
- [3] BAGNOLI P. E., BEVERINI N., FALCIAI R., MACCIONI E., MORGANTI M., SORRENTINO F., STEFANI F. and TRONO C., *J. Opt. A*, **8** (2006) S535.
- [4] BAGNOLI P. E., BEVERINI N., BOUHAEF B., CASTORINA E., FALCHINI E., FALCIAI R., FLAMINIO V., MACCIONI E., MORGANTI M., SORRENTINO F., STEFANI F. and TRONO C., *Nucl. Instrum. Methods Phys. Res. A*, **567** (2006) 515.
- [5] FERRARO P. and DE NATALE G., *Opt. Lasers Eng.*, **37** (2002) 115.
- [6] ARIE A., LISSAK B. and TUR M., *J. Lightwave Technol.*, **17** (1999) 1849.
- [7] CHOW J. H., LITTLER I. C., MCCLELLAND D. E. and GRAY M. B., *Opt. Lett.*, **30** (2005) 1923.
- [8] CHOW J. H., LITTLER I. C., MCCLELLAND D. E. and GRAY M. B., *Opt. Express*, **14** (2006) 4617.
- [9] BALL G. A. and GLENN W. H., *J. Lightwave Technol.*, **10** (1992) 1338.
- [10] KERSEY A. D., DAVIS M. A., PATRICK H. J., LEBLANC M., KOO K. P., ASKINS C. G., PUTNAM M. A. and FRIEBELE E. J., *J. Lightwave Technol.*, **15** (1997) 1442.
- [11] OTHONOS A., *Rev. Sci. Instrum.*, **68** (1997) 4309.
- [12] KERSEY A. D., *Opt. Fiber Technol.*, **2** (1996) 291.
- [13] BEVERINI N., MACCIONI E., MORGANTI M., STEFANI F., FALCIAI R. and TRONO C., *J. Opt. A*, **9** (2007) 958.
- [14] KERSEY A. D., BERKOFF T. A. and MOREY W. W., *Electron. Lett.*, **28** (1992) 236.
- [15] MELLE S. M., ALAVIE A. T., KARR S., COROY T., LIU K. and MEASURES R. M., *IEEE Photonics Technol. Lett.*, **5** (1993) 263.
- [16] KIRKENDALL C. K. and DANDRIDGE A., *J. Phys. D*, **37** (2004) R197.
- [17] WANSER K. H., *Electron. Lett.*, **28** (1992) 53.
- [18] ZUMBERGE M. A. and WYATT F. K., *Pure Appl. Geophys.*, **152** (1998) 221.